

Appearance of phenotypic plasticity of leaves in psammophyte *Corynephorus canescens* during flooding

 Olena Nedukha

Department of Cell Biology and Anatomy, M.G. Kholodny Institute of Botany, National Academy of Sciences of Ukraine, Tereshchenkivska str. 2, 01601 Kyiv, Ukraine; o.nedukha@hotmail.com

Received: 13.10.2021 | **Accepted:** 15.11.2021 | **Published online:** 21.11.2021

Abstract

The results of the study of the leaf structure in psammophyte *Corynephorus canescens*, which grew under controlled conditions and flooding using the methods of light microscopy, scanning electron microscopy, and laser confocal microscopy, are presented. This study revealed common and distinctive signs of morphological and anatomical parameters of *C. canescens* leaves in the phase of vegetative growth. Among the common features were the shape and size of the leaf laminas, hypostomatic type of the leaf, isolateral structure of the parenchyma, the thick-walled epidermis, and the bilayered hypodermis. Among the distinctive features were the signs of the destruction of cells in the photosynthetic parenchyma, change in their shape with the formation of protuberances at the cells' poles, and almost doubling area of the aerenchyma in *C. canescens* leaves under flooding conditions. Scanning electron microscopy showed the similarity of ultrastructure and density of trichomes on the adaxial surface, excepting the formation of cuticular wax structures on the epidermal surface of the leaves in flooded plants. The subcellular localization of silicon inclusions was studied for the first time. The presence of amorphous and small crystalline silicon inclusions in the periclinal walls of the main epidermal cells and amorphous silicon inclusions in leaf trichomes was established. An increase in the relative silicon content along the trichomes in the leaves' epidermis after flooding was revealed. It was assumed that the phenotypic plasticity of *C. canescens*, is realized through the increasing area of aerenchyma in leaves and increasing silicon content in trichomes. Such plasticity helps to optimize both the oxygen balance of plants and water balance in flooded plants, thus increasing the species' resistance to prolonged flooding.

Keywords: *Corynephorus canescens*, leaf epidermis, flooding, aerenchyma

Funding: This research was supported partly by the theme N467 "Cellular and molecular mechanisms of phenotypic plasticity of psammophytes and heliophytes in contrast conditions of water regime" of the National Academy of Sciences of Ukraine.

Competing Interests: The author claims that there is no conflict of interest regarding the research, authorship and/or publication of this article.

Introduction

The plants growing on sandy soils in steppe and desert areas and on the sandy shores of seas, rivers, and lakes are psammophytes. The study of morphological and anatomical

features of psammophytes is important for the understanding of the plant adaptation and response to various external influences (Hameed et al., 2009; Elhalim et al., 2016). It is known that the vegetation of coastal sandy dunes is constantly exposed to repeated

environmental stresses, which directly affects the survival and distribution of plant species. The most significant ecological stresses for psammophytes are drought, salinity, solar radiation, high intensity of light, low nutrient availability, and soil instability (Grigore & Toma, 2007; Bagousse-Pinguet et al., 2013). Mentioned factors closely interact as abiotic modulators of leaf adaptation and are directly regulated by primary stress signals, which trigger the appropriate structural and functional adaptation mechanism required for plant survival (Catoni & Gratani, 2013). Psammophytes growing on sandy dunes have developed mechanisms of resistance and adaptation to environmental changes (Ashraf & Harris, 2013; Ruocco et al., 2014; Futorna et al., 2017).

The morphological and anatomical features of the psammophytes' adaptation to environmental conditions are: the decrease of the leaves' size, the formation of water-storing parenchyma, changes in the foliar vascular system size, leaf laminae twisting, changes in stomatal density, increased indumentum, thickened cuticles, and synthesis of calcium inclusions in cells and intercellular spaces (Hameed et al., 2009; Elhalim et al., 2016; Jianu et al., 2021). Recently, silicon inclusions were found to be associated with plant resistance to changes in cell water balance. Notably, during drought, silicon enhances the suberization of the sclerenchyma of rice roots and lignification of the foliar epidermis of heliophyte *Phragmites australis* (Cav.) Trin. ex Steud. (Fleck et al., 2011; Nedukha & Kordyum, 2019). Psammophytes, in addition to the above-mentioned environmental stresses, may be affected by short-term or prolonged flooding. However, the adaptability of psammophytes to flooding has not been investigated.

Water is one of the main factors supporting the growth, development, and productivity of such psammophyte as *Corynephorus canescens* (L.) P. Beauv. (Poaceae). Considering that aerenchyma and epidermis of the leaves are principal tissues regulating the water balance of the plant (Kerstiens, 2006; Hansen et al., 2007), our work aimed to investigate in *C. canescens*: 1) the general anatomical structure of the leaves; 2) the epidermal ultrastructure of the leaves under different water supply conditions; 3) the location and content of silicon in the foliar epidermis to

understand the role of this element in the plant adaptation to flooding.

Material and methods

The leaves of two study variants of *C. canescens* (grown on slightly moist sandy soil and flooded for 21 days) were investigated. At the end of May, the turf of 30-days plants of *C. canescens*, which grew on sandy soil (Fig. 1 A), was planted in cups filled with river sand. In total, six cups containing 17 plants per cup were obtained. Three cups were flooded (Fig. 1 B) to the level of plants' hypocotyl. The other three cups with plants were not flooded and served a control. The duration of daylight for all six sampling series was from 16 h 8 m to 16 h 26 m, with daytime temperature 22–28 °C and nighttime temperature 20–23 °C. The control plants were watered every two days with 15 ml of settled running water. Standard biochemical methods were applied to determine and control the relative water content of the soil (Ermakov, 1982).

The histological slides were prepared following standard methods for cytological studies of the leaf structure under the light and scanning electron microscopy (Pausheva, 1988). For the light microscopy, the samples were fixed with a mixture of 2% paraformaldehyde and 2% glutaraldehyde (1:1, vol.) for 12 h, dehydrated with alcohol and acetone, and saturated with a mixture of epoxy resins (epon-araldite) (Pausheva, 1988). Sections (10 µm thick) were stained with 0.05% toluidine blue O and 0.01% safranin following Schmid (1980), and then studied with a light microscope Carl Zeiss NF (Germany). For scanning electron microscopy, samples were fixed in a mixture of aldehydes and dehydrated, fixed on special stubs, sputter-coated with gold, and studied under an electron microscope Jeol JSM 6060 LA (Japan). For cytochemical studies of the localization of silicon inclusions, clippings from the middle part of the leaf laminae were examined on a laser confocal microscope Zeiss LSM5 (Germany) using an excitation wavelength of 480 nm and emission of 530 nm. The fluorescence intensity of silicon was determined by the Pascal program (Zeiss, Germany).

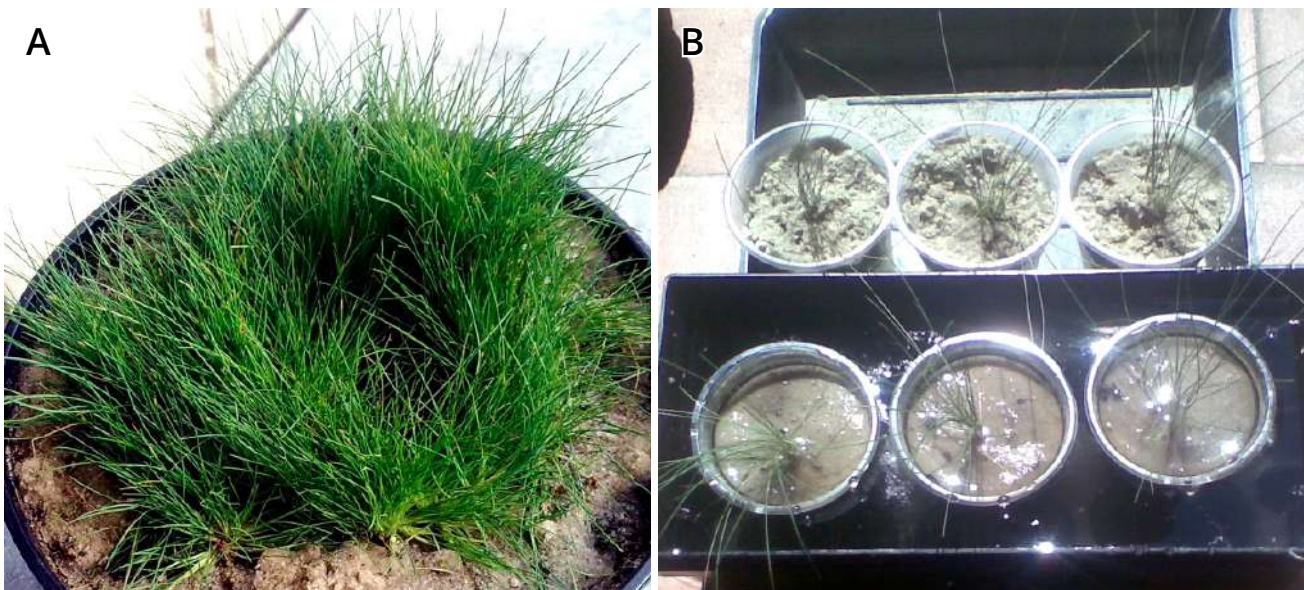


Figure 1. Study variants of *Corynephorus canescens*: **A** – general view of plants grown 30 days in semi-sandy soil, the phase of vegetative growth; **B** – plants transplanted into the sandy soil and serving a control variant (the top row) and flooded plants serving an experiment variant (the bottom row).

Results

The leaves of *C. canescens* in both sampling series were characterized by identical morphological structure (Fig. 1). In particular, leaves were sessile, simple, linear, twisted, hard, gray-green, with a rough surface and parallel venation. Their size in the rolling state was 130.0 ± 3.1 mm on the long axis and 2.7 ± 0.3 mm on the short axis. Their size on the short axis in the unwind state of leaf blade was from 7.3 ± 1 mm to 12.0 ± 2 mm. The anatomical structure of the leaves showed some differences between the variants that are described below.

Light microscopy

Control variant. The plants of *C. canescens* grown without flooding (control conditions) had twisted leaves with hippocrepiform cross-sections (Fig. 2 A). The upper (adaxial) leaf surface was uniform. The lower (abaxial) leaf surface had hollows and protrusions (Fig. 2 A, B). The protrusions were located near the vascular bundles. The sizes of epidermis and mesophyll cells differed among the surfaces (Table 1).

The thickness of the leaf lamina in the area of protrusions ranged from 237 ± 13 μ m (in the center of the lamina) to 200 ± 11 μ m (in the periphery of leaf lamina). The thickness

of the leaf lamina in the depressions was from 150 ± 10 μ m to 200 ± 13 μ m, respectively. Leaf laminae were hypostomatic with the isolateral structure of the parenchyma, thick-walled epidermis, and bilayered hypodermis containing inclusions.

The cells of the adaxial epidermis were thick-walled. The thickness of the cell walls in the adaxial epidermis was 3.2 ± 0.2 μ m, the height of the cells was 13.5 ± 1.1 μ m, and the width was 16.0 ± 1.3 μ m.

Behind the epidermis, depending on the cut and the surface area, were present one or two layers of thick-walled hypodermal cells. The thickness of the cell walls in the hypodermal cells was 2.7 ± 0.1 μ m; the average cell diameter was 7.1 ± 0.1 μ m. Occasionally, in hypodermal cells, the inclusions of various forms were visible.

Elongated, compacted, thin-walled mesophyll cells were located behind the hypodermis. The height of such cells was 27.3 ± 3.1 μ m, width – 10.7 ± 0.7 μ m. The average number of chloroplasts per section of the mesophyll cell was 11 ± 1.2 units. Four-six layers of rounded (diameter 12.2 ± 1.1 μ m) and slightly elongated (long axis – 15.4 ± 2.1 μ m, short axis – 11.2 ± 1.3 μ m) cells were situated below the initial mesophyll.

Between the mesophyll layers, small air cavities representing aerenchyma were visible. It extended to the abaxial epidermis. The

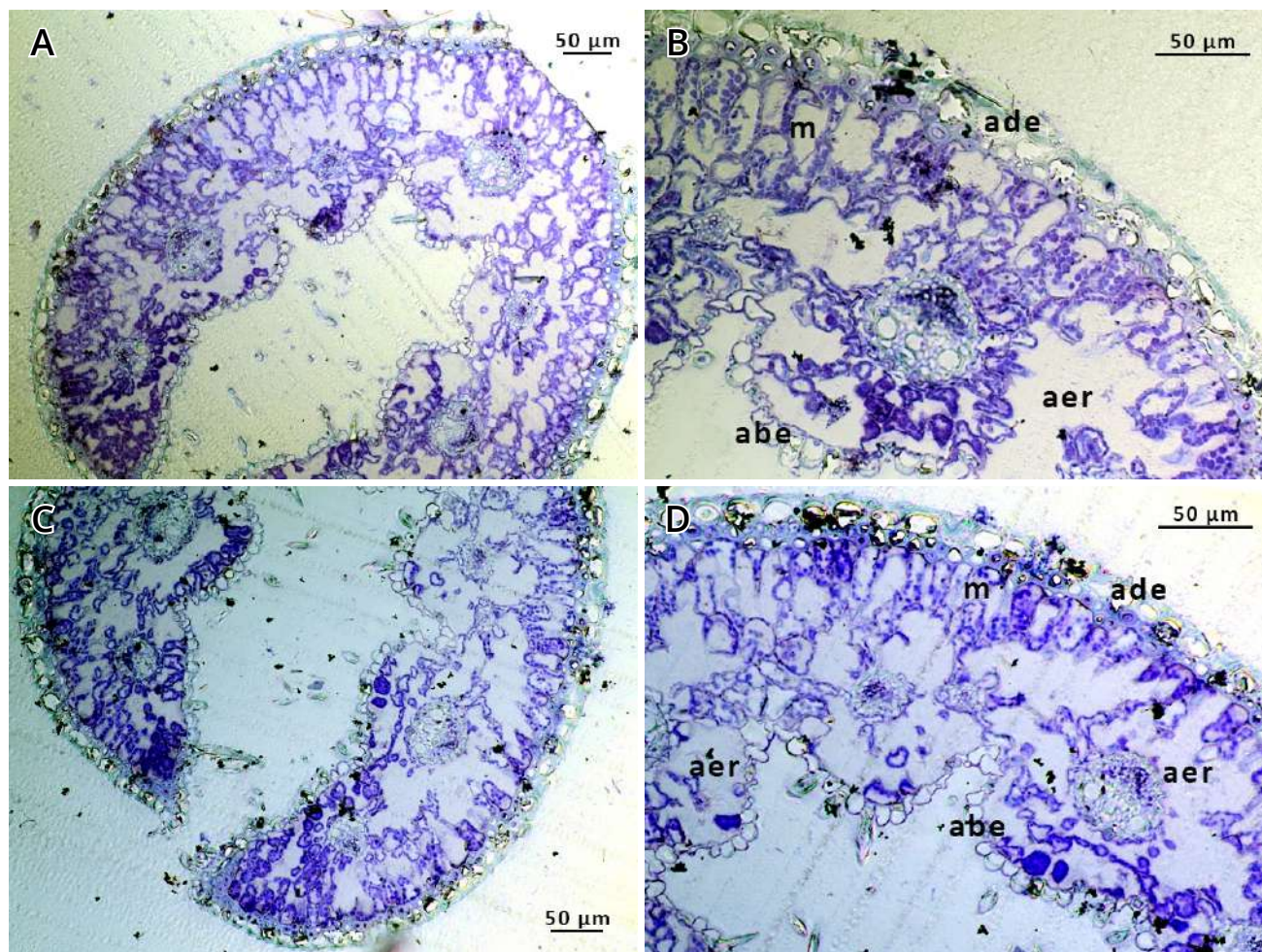


Figure 2. Cross-sections of the middle part of *Corynephorus canescens* leaf lamina: A, B – control variant; C, D – after 21 days of flooding. *abe* – abaxial epidermis; *ade* – adaxial epidermis; *aer* – aerenchyma; *m* – mesophyll.

aerenchyma area was $21.1 \pm 0.7\%$ of the total area of the leaf lamina cross-section.

The cells of the abaxial epidermis were almost rectangular. The average height of the cells was $11.7 \pm 1.1 \mu\text{m}$, the width – $10.8 \pm 0.4 \mu\text{m}$. The cell walls in abaxial epidermis were thinner than in the adaxial one, and their thickness was about $0.9 \pm 0.1 \mu\text{m}$ only. Between the cells of the abaxial epidermis, the guard cells of the stomata were present. On the surface of the abaxial epidermis, long transparent trichomes were visible.

The cross-section of the leaf lamina had seven vascular bundles: one large in the center (diameter was about $52 \mu\text{m}$) and six smaller (diameter was about $10 \mu\text{m}$) on the sides.

Flooded variant. 21-day flooding of *C. canescens* planted on sandy soil (with soil moisture of $70.6 \pm 2.3\%$) did not affect the morphology of leaf laminae but caused

changes in their anatomical structure. After 14 days of flooding, every fifth leaf changed its color from green to brown. After 21 days, the number of brown dead leaves increased.

We used for the anatomical investigations the leaves that remained green after 21-day flooding. We did not reveal the changes in the structure of epidermal and subepidermal (hypodermal) cells. However, we noted the changes in the size and shape of mesophyll cells (Table 1; Fig. 2 B, C). Cells of the upper mesophyll layer changed their shape and density. The shape of mesophyll cells changed from elongated to uneven with the protuberances on cell poles. The density of mesophyll cells decreased. The large intercellular spaces (aerenchyma) emerged between the cells of the upper mesophyll layer and extended from adaxial to abaxial epidermis. Hence, the area of the aerenchyma increased compared to the

Table 1. Physiological and structural parameters of *Corynephorus canescens* leaves.

Parameter	Control (soil moisture – 42.7±2.1%)	21-day flooding (soil moisture – 70.6±2.3% *)
Leaf shape	Linear	Linear
Leaf sizes:		
long axis, mm	13.0±1.3	13.0±1.1
short axis (in rolling state), mm	2.7±0.3	2.8±0.2
Area of aerenchyma on the leaf cross-section, %	21.1± 0.7	35.0±2.9 *
Sizes of adaxial epidermis cells:		
width, µm	16.0±1.3	16.0±1.3
height, µm	13.5±1.1	13.7±1.1
Diameter of hypodermal cells, µm	7.1±0.1	7.1±0.2
Sizes of mesophyll cells:		
first layer		
width, µm	10.7±0.7	12.5±1.1
height, µm	27.3±3.1	17.0±1.3 *
second–sixth layers		
width, µm	11.2±1.1	10.2±1.4
height, µm	15.4±2.1	13.4±2.1
Sizes of abaxial epidermis cells:		
width, µm	10.8±0.4	10.8±0.4
height, µm	11.7±1.1	11.7±1.1
Density of trichomes in adaxial epidermis per 1 mm ² (SEM)	314±27	342±31
Size of trichomes in adaxial epidermis:		
basal width, µm	15.3±2.2	15.7±1.7
height, µm	60.0±1.3	57.1±3.1
Density of trichomes in abaxial epidermis per 1 mm ² (SEM)	900±27	879±71
Size of trichomes in abaxial epidermis:		
basal width, µm	13.0±1.2	13.0±1.2
height, µm	76.0±7.1	73.0±7.9
Content of silicon inclusions in the cells of adaxial epidermis (LCM):		
at the base of trichomes, in relative units	98.0±3.1	89.7±3.5
along the trichome, in relative units	64.7±0.3	105.7±7.3 *
in the main epidermal cells, in relative units	51.5±0.9	46.3±1.2

Note. * – $p < 0.05$ (two-way ANOVA); SEM – scanning electron microscopy data; LCM – laser confocal microscopy data.

control, and occupied 35.0±2.9% of the cross-sectional area of the leaf lamina.

Scanning electron microscopy

Control variant. The plants of *C. canescens*, which grew in the control conditions, had irregular epidermis with protrusions of the

periclinal walls of the main epidermal cells located along adaxial surface of the leaf lamina. Whole epidermal cells were covered with a solid layer of cuticular wax depositions. The apexes of trichomes were oriented in one direction – from the leaf base to its tip (Fig. 3 A). Trichomes were short, with the rectangular or slightly oval shape of the base

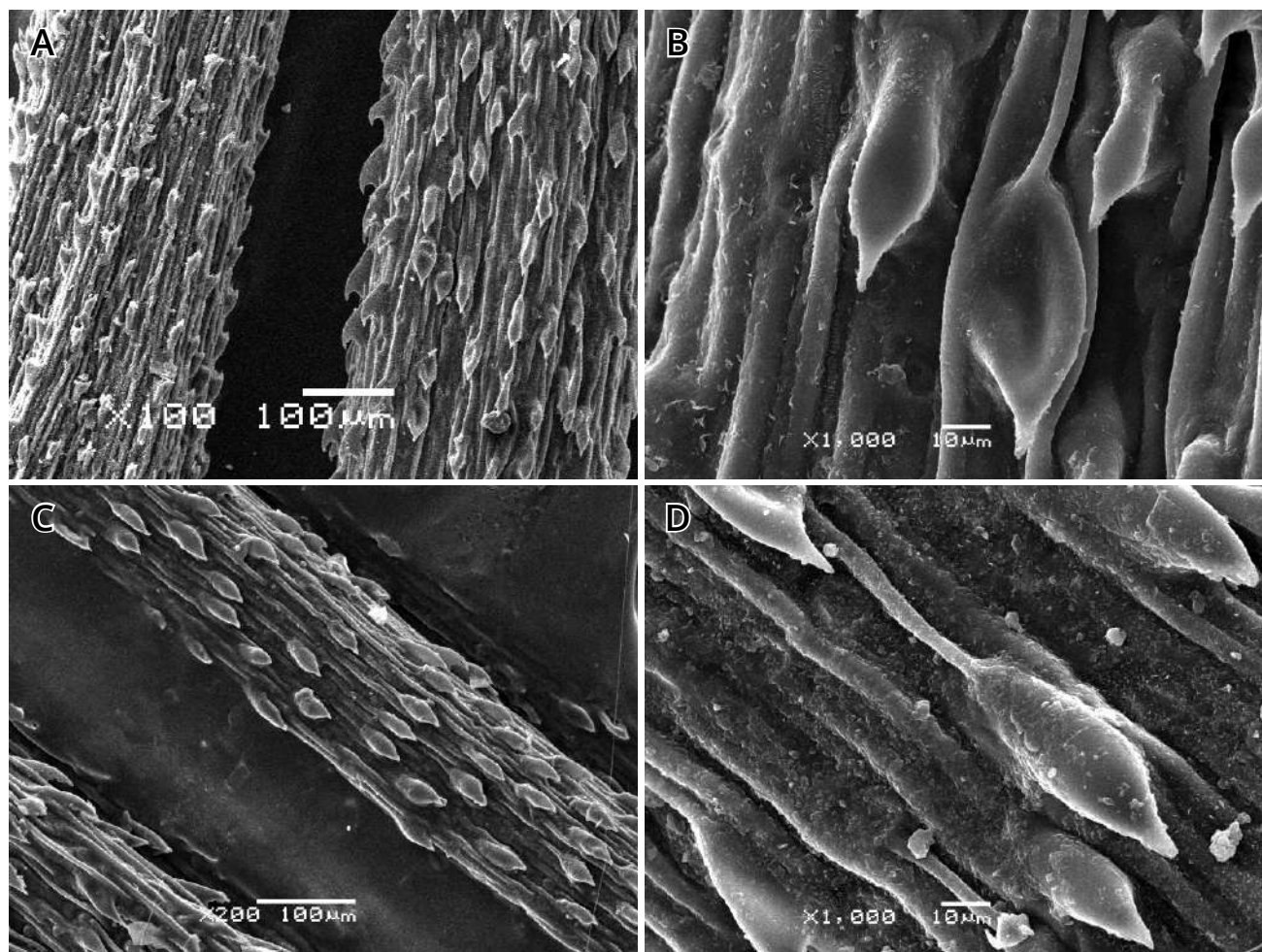


Figure 3. Ultrastructure of the adaxial surface of the leaves in *Corynephorus canescens* grown under control (A, B) and flooded (C, D) conditions.

and a hook-shaped apex (Fig. 3 B). The length of trichomes was $60.0 \pm 1.3 \mu\text{m}$, the base width - $15.3 \pm 2.2 \mu\text{m}$, the trichomes' middle part width - $30.0 \pm 2.2 \mu\text{m}$, the length of trichomes' hook - $10.0 \pm 1.3 \mu\text{m}$. The trichomes' surface was slightly smooth, similar to the surface of the surrounding cells. The average density of trichomes on the upper epidermis of the leaf was 314 ± 27 trichomes per 1 mm^2 (Table 1). Trichomes were situated in parallel rows; the distance (in one row) between them varied from 50 to $100 \mu\text{m}$.

The abaxial surface of the leaf was characterized by zonality (Fig. 4 A, B). It had alternated zones with longitudinally oriented trichomes and stomata. The width of each zone was about $100 \mu\text{m}$. Trichome areas raised above the stomata zones and covered them. The length of saber-like trichomes was $76.0 \pm 7.1 \mu\text{m}$, the width of the trichomes' base was $13.0 \pm 1.2 \mu\text{m}$. The average density of trichomes was 900 ± 27 trichomes per 1 mm^2 .

Trichomes were placed in parallel rows, and the distance (in one row) between trichomes varied from 50 to $100 \mu\text{m}$. The stomata raised above the epidermal surface and were arranged in rows. The average size of the stomatal guard cell was $30 \pm 1.5 \times 6.1 \pm 1.1 \mu\text{m}$. The distance between the stomata in one row varied from 80 to $145 \mu\text{m}$; the distance between stomatal rows was up to $20 \mu\text{m}$. The type of stomata cannot be clearly determined due to the presence of continuous cuticular-waxy inclusions on the cells surrounding the stomata.

Flooded variant. *Corynephorus canescens* plants, which were flooded for 21 days, showed ultrastructure of the epidermis identical with control samples (Fig. 3 C, D). In particular, short trichomes were arranged in the same longitudinal rows. The shape and size of trichomes were similar to those in the control samples (Table 1).

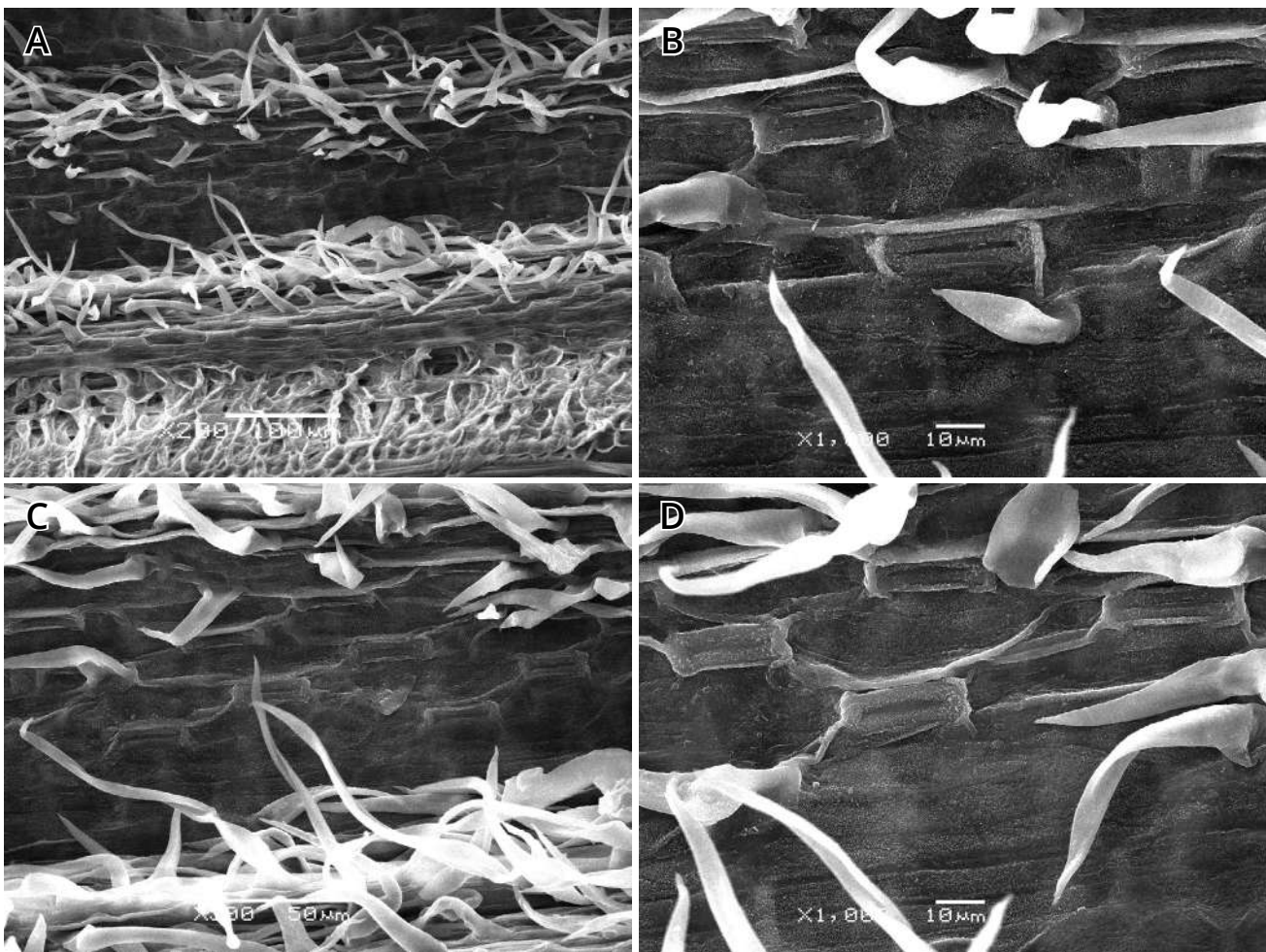


Figure 4. Ultrastructure of the abaxial surface of the leaves in *Corynephorus canescens* grown under control (A, B) and flooded (C, D) conditions.

On the adaxial leaf surface, only certain features were found in flooded plants. In particular, we detected verrucous structures on the surface of the main epidermal cells and at the base of trichomes (Fig. 3 D). The average density of trichomes on the adaxial leaf surface was 342 ± 31 per 1 mm^2 . Trichomes were also arranged in rows; the distance (in one row) between them varied from 50 to $120 \mu\text{m}$. Trichomes were short, similar in shape to those in the control variant, slightly oval at the base (top view), and had hook-shaped tips (well-visible in the side view). Trichomes' length was $57.0 \pm 3.1 \mu\text{m}$, the width of the trichomes' base was $15.0 \pm 1.7 \mu\text{m}$; the width of trichomes' middle part was $30 \pm 2.2 \mu\text{m}$; the length of trichomes' hook was $10.0 \pm 1.3 \mu\text{m}$. Occasionally the surface of the main epidermal cells was covered with waxy structures of various shapes.

No differences were detected regarding the control variant on the abaxial leaf surface of

flooded *C. canescens* plants (Fig. 4 C, D). The abaxial leaf surface was characterized by the presence of identical trichomes and zonality with similar trichomes and elongated stomata.

Localization of silicon inclusions

Control variant. Laser confocal microscopy allowed us to determine the localization of silicon inclusions in the leaves of *C. canescens*. An evident green fluorescence of silicon inclusions in the adaxial epidermis was detected in the control plants (Fig. 5 A).

Silicon inclusions were present in the form of small bodies of rounded or irregular shape (at the base of trichomes) and fine-grained amorphous inclusions smaller than 10 nm (along the trichomes and in the main epidermal cells). The luminescence intensity of silicon bodies and amorphous silicon inclusions differed in the trichomes and main epidermal cells (Table 1; Fig. 5 C, C'). At the base

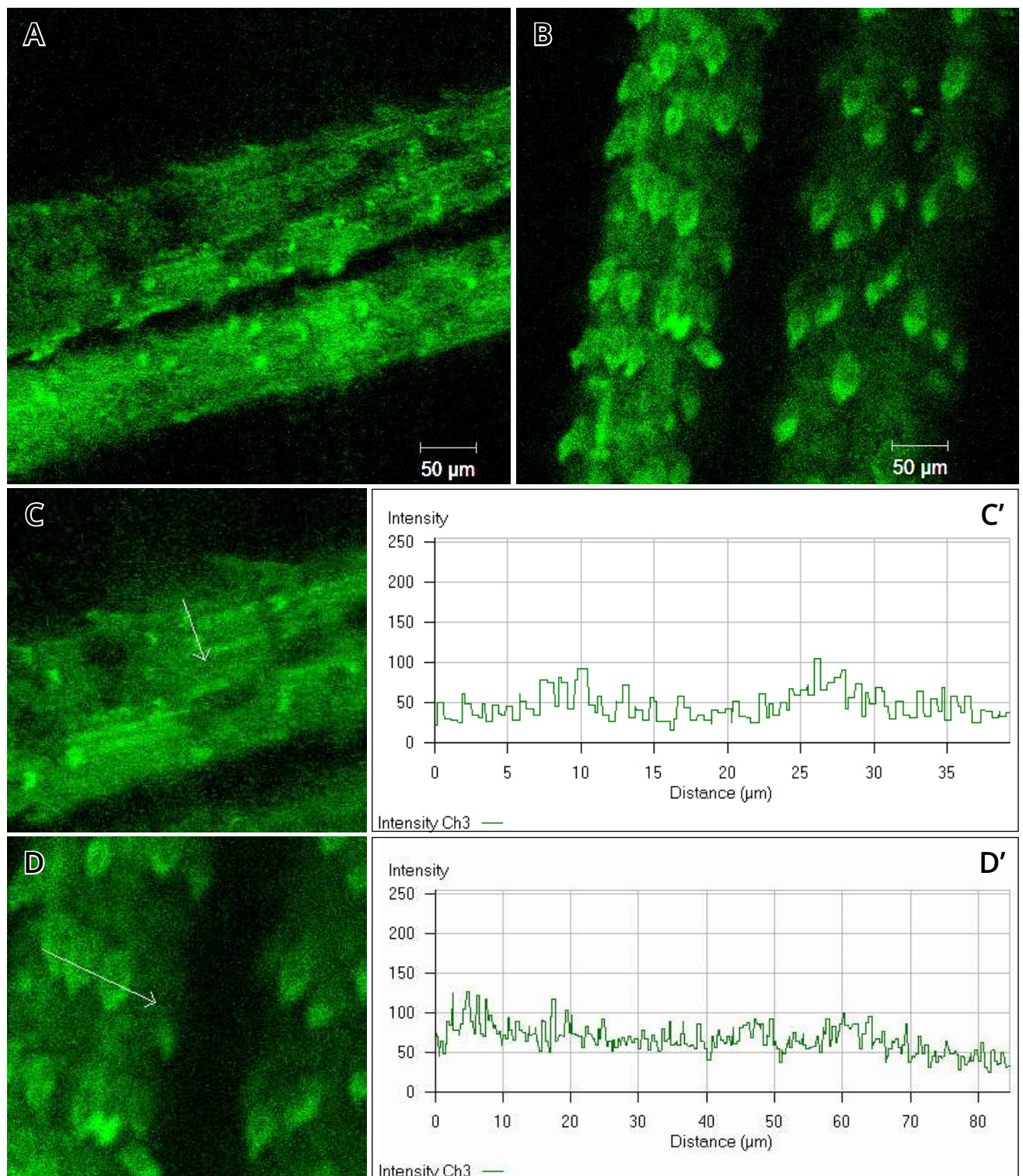


Figure 5. Microphotographs of silicon inclusions fluorescence in the leaves of control (A, C) and flooded (B, D) plants of *Corynephorus canescens*. C' and D' – histograms of silicon fluorescence intensity scanned from the photos C and D (white arrows indicate precise locations); ordinate – silicon fluorescence intensity (in relative units), abscissa – distance (in µm) scanned from the Figures C and D.

of the trichomes, the fluorescence intensity of silicon bodies was the highest.

Flooded variant. In flooded plants, the green fluorescence of silicon inclusions on the

adaxial surface was similar to that in control samples (Fig. 5 B). Silicon inclusions in the form of grains were found both at the base of the trichomes and along their entire cell, as well as on the surface of the main epidermal

cells surrounding the trichomes. The level of silicon fluorescence in flooded *C. canescens* plants is presented in Table 1 and Fig. 5 D, D'. Comparative analysis of luminescence intensity showed that flooding increased the silicon content in trichomes.

Discussion

Thus, *C. canescens* had the same shape of leaves (horseshoe-shaped cross-sections) and their twisting regardless of the growing conditions. Twisting and/or folding of leaves is a sign of many psammophytes irrespective of their place of growth (Ripley & Redmann, 1976; Perrone et al., 2015), which is reflected in the specialized structure of their leaf lamina tissues. Change of the leaf shape helps the plant to reduce water consumption during increasing external temperature. It optimizes water and energy balances, responding to changes in heat capacity, and the conductivity of water vapor and carbon dioxide (Redmann, 1985).

We found that three weeks of flooding of *C. canescens* plants caused a 1.7-time increase in the leaves' aerenchyma area compared to the control. Although the aerenchyma in flooded plants occupied almost 35% of the leaf area, its structure was the same as in typical plants. Formed aerenchyma provided more oxygen to the plant and helped in its resistance against flooding. A similar effect is reported for many cultivated and wild plant species in the condition of prolonged flooding (Vartapetian & Jackson, 1997; Evans, 2004; Parlanti et al., 2011). Therefore, we can conclude that psammophyte *C. canescens* can withstand prolonged flooding.

We found a high density of cuticular-wax depositions on the periclinal walls of epidermal cells and the presence of non-glandular trichomes on the adaxial surface of *C. canescens* leaves. Non-glandular trichomes protect the aboveground plant's organs from insects and herbivores, as well as from mechanical damage (Peter et al., 1995). The increase in trichomes density also occurs during drought (Bourland et al., 2003). Dense pubescence changes the optical properties of the leaf surface and can reflect or absorb the light of specific wavelengths. In addition, trichomes hold an air layer on the leaf surface,

which helps preserve heat and moisture (Peter et al., 1995).

In epidermal and hypodermal cells of *C. canescens* leaves, regardless of growth conditions, we detected the presence of inclusions of different shapes and sizes. It is reported that these inclusions contain calcium and potassium, and granular inclusions can be of varying nature (Daniela et al., 2009; HuaCong et al., 2010). Calcium oxalate crystals, like silicon inclusions, attract water molecules, reducing water loss of the plant cells (Zhan-Yuan, 2000).

The presence of silicon inclusions in *C. canescens* cells was proved by laser confocal microscopy. In *C. canescens*, silicon inclusions were found in the main epidermal cells and trichomes of the adaxial leaf surface, regardless of growth conditions. According to the literature, such silicon inclusions represent a biological form of the silicon ions connection with proteins, amino acids, lipids or polysaccharides (Müller & Grachev, 2009). Silicon ions are often found in combination with polysaccharides in cell walls, and such structures, in general, are called silicon inclusions (Lins et al., 2002; Guerriero et al., 2016; Grasik et al., 2020). We proved the presence of silicon ions in such inclusions using the Pascal program (with laser confocal microscopy).

Silicon improves the luminous flux characteristics by keeping the leaf laminae in a folded state, optimizing photosynthetic processes (Ma et al., 2011). This also reduces the heat load due to efficient far-infrared heat dissipation of silica, which provides a passive cooling mechanism for folded leaves during the intense insolation (Wang et al., 2005). Thus, the obtained data indicate the phenotypic plasticity of psammophyte *C. canescens* realized under the influence of adverse factors.

Conclusions

The peculiarities of anatomy and surface ultrastructure of the leaf laminae in psammophyte *C. canescens* were revealed. The localization and content of silicon inclusions were investigated using laser confocal microscopy. It was found that the three-week flooding of *C. canescens* plants during

the vegetative growth phase increased the content of aerenchyma in their leaves and stimulated the formation of wax depositions on the adaxial foliar epidermis, and increased the content of silicone inclusions in foliar trichomes.

Acknowledgements

We are grateful to Professor D.V. Dubina (Institute of Botany of NASU), who passed *C. canescens* seeds to the Department of Anatomy and Cell Biology for research. We are also grateful to Professor, Corresponding Member of NASU, Elizabeth L. Kordyum (Institute of Botany of NASU) for reviewing the manuscript of the article.

References

- Ashraf, M. A., & Harris, P. J. (2013). Photosynthesis under stressful environments: an overview. *Photosynthetica*, 51(2), 163–190. <https://doi.org/10.1007/s11099-013-0021-6>
- Bagousse-Pinguet, Y. L., Forey, E., Touzard, B., & Michalet, R. (2013). Disentangling the effects of water and nutrients for studying the outcome of plant interactions in sand dune ecosystems. *Journal of Vegetation Science*, 24(2), 375–383. <https://doi.org/10.1111/j.1654-1103.2012.01462.x>
- Bourland, F. M., Hornbeck, J. M., McFall, A., & Calhoun, S. (2003). Breeding & genetics. A rating system for leaf pubescence of cotton. *The Journal of Cotton Science*, 7, 8–15.
- Catoni, R., & Gratani, L. (2013). Morphological and physiological adaptive traits of Mediterranean narrow endemic plants: the case of *Centaurea gymnocarpa* (Capraia Island, Italy). *Flora*, 208(3), 174–183. <https://doi.org/10.1016/j.FLORA.2013.02.010>
- Daniela, C., Forino, L. M., Balestri, M., & Pagni, A. M. (2009). Leaf anatomical adaptations of *Calystegia soldanella*, *Euphorbia paralias* and *Otanthus maritimus* to the ecological conditions of coastal sand dune systems. *Caryologia*, 62(2), 142–151. <https://doi.org/10.1080/00087114.2004.10589679>
- Elhalim, M. E., Abo-Alatta, O., Habib, S. A., & Elbar, O. H. (2016). The anatomical features of the desert halophytes *Zygophyllum album* L.F. and *Nitraria retusa* (Forssk.) Asch. *Annals of Agricultural Sciences*, 61(1), 97–104. <https://doi.org/10.1016/j.AOAS.2015.12.001>
- Ermakov, A. I. (1982). Determination of water content and active acidity plant objects. In: A. Ermakov (Ed.), *Methods of biochemical research of plants* (pp. 20–35). Agropromizdat. (In Russian)
- Evans, D. E. (2004). Aerenchyma formation. *New Phytologist*, 161(1), 35–49. <https://doi.org/10.1046/j.1469-8137.2003.00907.x>
- Fleck, A. T., Nye, T., Repenning, C., Stahl, F., Zahn, M., & Schenk, M. K. (2011). Silicon enhances suberization and lignification in roots of rice (*Oryza sativa*). *Journal of Experimental Botany*, 62(6), 2001–2011. <https://doi.org/10.1093/jxb%2Ferq392>
- Futorna, O. A., Badanina, V. A., & Zhygalova, S. L. (2017). Ecological-anatomical characteristics of some *Tragopogon* (Asteraceae) species of the flora of Ukraine. *Biosystems Diversity*, 25(4), 274–281. (In Ukrainian). <https://doi.org/10.15421/011742>
- Grasik, M., Sakovic, D., Abram, K., Vogel-Mikus, K., & Gaberscik, A. (2020). Do soil and leaf silicon content affect leaf functional traits in *Deschampsia caespitosa* from different habitats? *Biologia Plantarum*, 64, 234–243. <https://doi.org/10.32615/bp.2019.155>
- Grigore, M. N., & Toma, C. (2007). Histo-anatomical strategies of Chenopodiaceae halophytes; adaptive, ecological and evolutionary implications. *WSEAS Transactions on Biology and Biomedicine*, 12(4), 204–218.
- Guerriero, G., Hausman, J. F., & Legay, S. (2016). Silicon and the plant extracellular matrix. *Frontiers in Plant Science*, 7, Article 463. <https://doi.org/10.3389/fpls.2016.00463>
- Hameed, B. H., Krishni, R. R., & Sata, S. A. (2009). A novel agricultural waste adsorbent for the removal of cationic dye from aqueous solutions. *Journal of Hazardous Materials*, 162(1), 305–311. <https://doi.org/10.1016/j.jhazmat.2008.05.036>
- Hansen, D. L., Lambertini, C., Jampeetong, A., & Brix, H. (2007). Clone-specific differences in *Phragmites australis*: effects of ploidy level and geographic origin. *Aquatic Botany*, 86(3), 269–279. <https://doi.org/10.1016/j.AQUABOT.2006.11.005>
- HuaCong, C., XingDong, H., Rong, L., Wei, W., PingPing, X., YuBao, G., & HaLin, Z. (2010). Characteristics of plant calcium fractions for 25 species in Tengger Desert. *Sciences in Cold and Arid Regions*, 2(2), 168–174.
- Jianu, L. D., Bercu, R., & Popoviciu, D. R. (2021). *Silene thymifolia* Sibth. et Sm. (Caryophyllaceae) – a vulnerable species in Romania: anatomical aspects of vegetative organs. *Notulae Botanicae Horti Agrobotanici Cluj-Napoca*, 13, Article 10875. <https://doi.org/10.15835/NSB13110875>

- Kerstiens, G. (2006). Water transport in plant cuticles: an update. *Journal of Experimental Botany*, 57(11), 2493–2499. <https://doi.org/10.1093/JXB%2FERL017>
- Lins, U., Barros, C. F., da Cunha, M., & Miguens, F. C. (2002). Structure, morphology, and composition of silicon biocomposites in the palm tree *Syagrus coronata* (Mart.) Becc. *Protoplasma*, 220, 89–96. <https://doi.org/10.1007/s00709-002-0036-5>
- Ma, J. F., Yamaji, N., & Mitani-Ueno, N. (2011). Transport of silicon from roots to panicles in plants. *Proceedings of the Japan Academy. Series B, Physical and Biological Sciences*, 87(7), 377–385. <https://doi.org/10.2183/pjab.87.377>
- Müller, W. E. G., & Grachev, M. (2009). *Biosilica in evolution, morphogenesis, and nanobiotechnology* (pp. 295–314). Springer.
- Nedukha, O. M., & Kordyum, E. L. (2019). Participation of silicon ions in the resistance of plants to lower soil moisture. *Reports of the National Academy of Sciences of Ukraine*, 7, 89–95. (In Ukrainian). <https://doi.org/10.15407/dopovidi2019.07.089>
- Parlanti, S., Kudahettige, N. P., Lombardi, L., Mensuali-Sodi, A., Alpi, A., Perata, P., & Pucciariello, C. (2011). Distinct mechanisms for aerenchyma formation in leaf sheaths of rice genotypes displaying a quiescence or escape strategy for flooding tolerance. *Annals of Botany*, 107(8), 1335–1343. <https://doi.org/10.1093/aob%2Fmcr086>
- Pausheva, Z. P. (1988). *A workshop on plant cytology*. Agropromizdat. (In Russian)
- Perrone, R., Salmeri, C., Brullo, S., Colombo, P., & Castro, O. D. (2015). What do leaf anatomy and micro-morphology tell us about the psammophilous *Pancreaticum maritimum* L. (Amaryllidaceae) in response to sand dune conditions? *Flora*, 213, 20–31. <https://doi.org/10.1016/J.FLORA.2015.03.001>
- Peter, A. J., Shanower, T. O., & Romeis, J. (1995). The role of plant trichomes in insect resistance: a selective review. *Phytophaga*, 7, 41–63.
- Redmann, R. E. (1985). Adaptation of grasses to water stress-leaf rolling and stomate distribution. *Annals of the Missouri Botanical Garden*, 72(4), 833–842. <https://doi.org/10.2307/2399225>
- Ripley E. A., & Redmann R. F. (1976). Grasslands. In: J. L. Monteith (Ed.), *Vegetation and the atmosphere*. Vol. 2. Case studies. Academic Press.
- Ruocco, M., Bertoni, D., Sarti, G., & Ciccarelli, D. (2014). Mediterranean coastal dune systems: which abiotic factors have the most influence on plant communities? *Estuarine Coastal and Shelf Science*, 149(5), 213–222. <https://doi.org/10.1016/J.ECSS.2014.08.019>
- Schmid, R. (1980). Comparative anatomy and morphology of *Psiloxylon* and *Heteropuxis* and subfamilial and tribal classification of Myrtales. *Taxon*, 29(5/6), 559–595.
- Vartapetian, B. B., & Jackson, M. B. (1997). Plant adaptations to anaerobic stress. *Annals of Botany*, 79(Suppl. A), 3–20. <http://www.jstor.org/stable/42764824>
- Wang, L., Nie, Q., Li, M., Zhang, F., Zhuang, J., Yang, W., Li, T.J., & Wang, Y. (2005). Biosilicified structures for cooling plant leaves: a mechanism of highly efficient midinfrared thermal emission. *Applied Physics Letters*, 87, Article 194105. <https://doi.org/10.1063/1.2126115>
- Zhan-Yuan, D. (2000). Anatomical observations on the photosynthetic branch of *Haloxylon ammodendrom* (C.A. Mey) Bunge and its character of drought and salt resistance. *Journal of Arid Land Resources and Environment*, 14, 70–83.

Прояв фенотипової пластичності листків псамофіту *Corynephorus canescens* при затопленні

Олена Недуха

Відділ клітинної біології та анатомії, Інститут ботаніки ім. М.Г. Холодного НАН України, вул. Терещенківська, 2, Київ, 01004, Україна; o.nedukha@hotmail.com

Наведено результати дослідження структури листків псамофіта *Corynephorus canescens*, що зростає в контрольованих умовах та при затопленні із використанням методів світлової мікроскопії, сканувальної електронної мікроскопії та лазерно-конфокальної мікроскопії. Дослідження морфо-анатомічних показників листків *C. canescens* у фазі вегетативного росту показало наявність спільних та відмінних ознак контрольних та затоплених зразків. Спільними ознаками були: форма та розміри

пластинок, гіпостоматичний тип пластинки та ізолатеральна структура паренхіми, товстостінний епідерміс та двошаровий гіподерміс. Відмінними показниками були: наявність ознак руйнації клітин фотосинтезуючої паренхіми, зміна їхньої форми з формуванням виростів на полюсах клітин та збільшення майже вдвічі площі аеренхіми у листках *C. canescens* при затопленні. Методом сканувальної електронної мікроскопії встановлена подібність ультраструктури та щільності трихом на адаксіальній поверхні за виключенням формування кутикулярно-воскових структур на поверхні епідермісу листків у затоплених рослин. Вперше вивчена субклітинна локалізація іонів кремнію та встановлена наявність аморфних і дрібних кристалічних включень кремнію у периклінальних стінках основних клітин епідермісу та аморфних включень кремнію – у трихомах листків. Виявлено підвищення відносного вмісту кремнію вздовж трихоми в епідермісі листків рослин після затоплення. Припускається, що фенотипічна пластичність *C. canescens*, що проявлялась у збільшенні площі аеренхіми в листках та підвищенні вмісту кремнію у трихомах, сприяє оптимізації як кисневого балансу рослин, так і водного статусу затоплених рослин, і таким чином підвищує стійкість досліджуваного виду до тривалого затоплення.

Ключові слова: *Corynephorus canescens*, епідерма листка, затоплення, аеренхіма